



## Application of Treated Iraqi Rice Husk as Adsorbent for Phosphate Removal from Aqueous Solution

Anaam A. Sabri<sup>a</sup>, Yaser A. Hashim<sup>b\*</sup>

<sup>a</sup> Chemical Engineering Dept., University of Technology, Baghdad, Iraq. [aaksabri@yahoo.com](mailto:aaksabri@yahoo.com)

<sup>b</sup> Chemical Engineering Dept., University of Technology, Baghdad, Iraq. [yaserengineer80@yahoo.com](mailto:yaserengineer80@yahoo.com)

\*Corresponding author.

Submitted: 01/01/2020

Accepted: 11/04/2020

Published: 25/11/2020

### KEYWORDS

Agricultural waste,  
Phosphate, Rice husk  
ash, Adsorbent,  
Adsorption isotherm.

### ABSTRACT

*In the present work, agricultural waste, (Iraqi rice husk A'anbar type) was developed with thermal and chemical treatments for using as an adsorbent to remove phosphate anion from aqueous solution and the thermal treatment at 500°C was the best.*

*Batch experiments were conducted to obtain the maximum removal of phosphate via changing the parameters of the process, such as contact time, pH, adsorbent dose, initial solute concentration, and the existence of competitive anions upon the removal of phosphate and was investigated. The adsorbent characterization was performed employing Fourier transform infrared (FTIR), X-ray fluorescence (XRF), scanning electron microscope (SEM), the BET surface area and pore volume, and X-ray diffraction spectrophotometric analysis (XRD).*

*The maximum removal of phosphate was achieved as (98.37 %), at contact time 140 min., pH 2.0, adsorbent dose 20 g/L, and initial concentration 5 mg/L at room temperature. The effects of competing ions of  $\text{CO}_3^{2-}$ ,  $\text{NO}_3^-$ , and  $\text{SO}_4^{2-}$  anions were studied. The experimental data manifested the best fit for the Langmuir isotherm model ( $R^2 = 0.99$ ) and the pseudo-second-order kinetic model ( $R^2 = 0.99$ ). Rice husk ash was found efficient for phosphate removal from the industrial wastewater and aqueous solutions.*

**How to cite this article** A. A. Sabri and Y. A. Hashim, "Application of Treated Iraqi Rice Husk as Adsorbent for Phosphate Removal from Aqueous Solution" Engineering and Technology Journal, Vol. 38, Part A, No. 11, pp. 1602-1617, 2020.

DOI: <https://doi.org/10.30684/etj.v38i11A.1538>

This is an open access article under the CC BY 4.0 license <http://creativecommons.org/licenses/by/4.0>

## 1. INTRODUCTION

Phosphorus is principally utilized in the agriculture sector as a fertilizer and in the households as a detergent, causing the phosphate release into the environment [1]. The phosphate existence in water is a consequence of the washing out natural operations from minerals and rocks, from the soil, in which the phosphorus compounds were inserted with the fertilizers and from the pollution with the

public or manufacturing waste. In surface and groundwater water, the concentration of such compounds may be the change in a broad range from ( $10^{-3}$ ) mg to a few milligrams of phosphate anion per liter. The excess of phosphate in water can participate in the water reservoirs eutrophication [2] enhancing plentiful growth of vegetation and zooplankton intense activity utilizing bigger quantities of oxygen ( $O_2$ ) which may affect on the aerobic organisms that live in the water. The result of such eutrophication is the water ecosystem's troubled equilibrium [3, 4]. The water eutrophication phenomenon is unwanted and risky, so the phosphate removal from the water is too significant.

Also, the phosphate leaching into the groundwater throughout the subsoil influences the quality of drinking water, such as a possible danger to the health for both the human and the animals [5-9]. The osteoporosis and the damage of the kidney have been documented being due to high phosphate concentration [10].

Phosphorus compounds can be removed via various techniques: precipitation, ion exchange, adsorption, coagulation, and microfiltration coagulation [11]. Presently, the utmost interests are the processes of adsorption due to the high efficiency, non-toxicity, ease, accessibility of a broad adsorbents range, and the likelihood of usage within a broad concentration range [2-4].

Different investigations have revealed the use of various agricultural waste materials as adsorbents for removal of phosphate from the wastewater, like the wheat residue [12], ground burnt patties [1], red seaweed [13], fruit juice residue [14], Eggshell ash [15], sugar cane [16], and Palm Kernel Shell [17] for the removal of phosphate from the wastewater.

The rice husk is an agricultural waste gained from the rice mill. The removal of the rice husk throughout the refining of rice produces a discarding difficultly owing to its less marketable worth. Also, the rice husk manipulating and transport is difficult owing to their less density. Plenty of produced rice from the treatment of rice is dumped or burnt like a waste. The rice husk that burns in the open fields results in health and environmental difficulties in the surrounding regions, particularly in the evolving countries. So, it's too significant to entirely use rice husk. The rice husk was washed properly using distilled water and heated at  $500^\circ\text{C}$  for 2 hours in muffle furnaces, then, the rice husk ash was then activated to modify the surface characteristics using HCL (1N). And for the chemically and heat treated adsorbent at  $500^\circ\text{C}$  with NaOH, the rice husk ash was then refluxed with 1N of NaOH for 24 h to remove the lignin-based substances and increase the specific surface area of the rice husk.

Care has been concentrated upon the use of the unmodified and modified rice husk-like an adsorbent for removal of different contaminants, [18] such as nitrate, sulfate, carbonate anion, etc. Recently, an effective and economical method for removal of phosphate anion by using rice husk as adsorbent which was burnt in the oven at  $500^\circ\text{C}$ . [19].

Since there are many studies have been conducted using the treatments of rice husk, such as acid, base, and thermal, but there is a little work concerning the treatment of rice husk by burning method, therefore the current investigation uses the Iraqi rice husk before and after treatment for removal of phosphate anion from the wastewater. Studies of the batch mode adsorption were achieved for studying the effects of different experimental parameters, namely contact time, pH, adsorbent dosage, as well as initial concentration.

## 2. USED MATERIAL AND PROCEDURES

### I. Adsorbent

An Iraqi rice husk (A'anbar type) was collected from AL-Meshkhab province in the south of Iraq, firstly, gained from a mill of rice mill and washed thoroughly with distilled water to remove adhering soil and clay then dried at  $110^\circ\text{C}$  for 24 hr. and finally dried at ( $110^\circ\text{C}$ ) for (24 h) [20]. Different treatments of rice husk were carried out as follows:

- 1) Thermal pretreatment: The rice husk was located on a ceramic plane surface, placed inside a furnace for heating at temperatures 300, 400, 500, 600, and  $700^\circ\text{C}$  at a rate of heating of ( $25^\circ\text{C}/\text{min}$ ) and a holding time of 2h to determine the optimum temperature. Then, the charred remainder was gathered and cooled to the room temperature. Depending on the above mention used temperatures, it was found that the best removal of phosphate anion occurred at  $500^\circ\text{C}$  in the present work.
- 2) Chemical pretreatment: The rice husk ash (burnt rice husk at  $500^\circ\text{C}$ ) was activated with HCL with normality (1N), the blend of HCL, and the rice husk ash (with a ratio of 1:1) was

reserved for (24) h with stirring at the room temperature. Then, rice husk ash was cleaned with the distilled water till pH 7.0 and again dried overnight at 110°C. [20]

- 3) Chemical pretreatment: The rice husk ash (burnt rice husk at 500 C°) was activated with NaOH with normality (1N), the blend of NaOH, and the rice husk ash (in ratio 1:1) was reserved for 24 hours with stirring at the room temperature. Then, the rice husk was cleaned with the distilled water up to pH 7.0 and again dried overnight at 110°C. [21]

## II. Reagents

The chemicals needed for the phosphate analytical determination in the aqueous solutions (ammonium molybdate, potassium dihydrogen phosphate, sulfuric acid, and hydrazine hydrate. (HCl) and (NaOH) pellets were utilized for the adjustment of (pH). The whole chemicals were of analytical grade.

## III. Adsorbate solution

The standard phosphate stock solution was made via a dissolving amount of  $\text{KH}_2\text{PO}_4$  in 1000 mL distilled water. The stock solution was more diluted for having the needed primary phosphate solution concentration.

## IV. Used Instruments

For the samples, the Fourier transform infrared spectra were recorded via (FTIR) spectroscope (Bruker – Tensor 27, Germany) employing KBr as a reference. The X-ray powder diffraction (XRD) tests were done with a diffraction unit (Shimadzu-6000, Japan). SEM instrument (TESCAN, Germany), was used to examine the morphology of adsorbent. X-ray fluorescence (SPECTRO, Germany) was utilized to analyze the composition of the adsorbent. A digital (pH) meter (LI 120, Elico India) was employed to measure the pH of the sample that was calibrated with standard buffer solutions having a (pH) of (4.0), (7.0), and (9.2). (U.V-1100, China) a spectrophotometer was utilized to obtain the phosphate solutions concentrations before and next to the adsorption for checking the perfect removal of phosphate.

## V. Batch Adsorption Techniques

Tests of adsorption were conducted batch-wise in (100 mL) conical flasks containing 50ml of phosphate solution ( $\text{KH}_2\text{PO}_4$ ) used as phosphate source and a fixed amount of adsorbent. The primary concentration was varying from 5 to 150 mg/L. Beyond a limited time of strong stirring (250 rpm) at the room temperature ( $298 \pm 2\text{K}$ ), a suspension was sifted by Whatman filter (No. 42) and the filtrate solution resulted was analyzed via (U.V-1100, China) spectrophotometer at (840 nm) for the content of phosphate by molybdenum blue method [22]. The experiments of the batch process were conducted which included the contact time, pH of the solution, adsorbent dosage, and initial concentration for whole adsorbents using the essential adsorbent and the (50) mL of the stock solution. Various primary concentrations (5–150 mg/L) of solutions of phosphate were made via an appropriate stock dilution of the phosphate solution, the pH solution (2-10) and modified via the adding (0.1 N) NaOH and (0.1 N) HCl solution, the needed quantity of adsorbent (2-40 g/L) was added, and the contents in flask were vibrated for the wanted time of contact (5-200) min.. these parameters were studied for the removal of phosphate from the aqueous solutions. The whole experiments were carried out at ( $298 \pm 2$ )K. Batch experiments were executed via blending a proper dose of adsorbent at constant vibrating speed (250 rpm). Flasks were removed at unvarying intervals of time, and the analysis of the sample was done via pursuing a standard method employing (UV–vis) spectrophotometer. The efficiency of phosphate removal efficiency was computed via this equation [14]:

$$\text{Phosphate removal (\%)} = \frac{c_o - c_f}{c_o} \times 100 \quad (1)$$

The capacity of adsorption (q) in (mg/g) was found via this equation:

$$\text{Adsorption capacity (q)} = \frac{(c_o - c_e)V}{w} \quad (2)$$

Where:

q : Capacity of adsorption, (mg/g).

$C_o$ ,  $C_f$  and  $C_e$ : The original, final and equilibrium concentrations (mg/L) of phosphate within the sample, correspondingly.

$W$  and  $V$ : The mass of adsorbent in (g) and volume of the adsorbate solution in (L), respectively.

### 3. RESULTS AND DISCUSSION

#### I. Adsorbent Characterization

The chemical structure of the adsorbent has vital importance in understanding the adsorption process. The FTIR technique is an important tool to identify the characteristic functional groups on the surface of the samples in the figure (1 a, b, c, and d), these are instrumental in the adsorption of the chemical compounds. The spectral range changed from (4000) to (400)  $\text{cm}^{-1}$ . The rice husk (RH), rice husk ash (RHA), after treatment rice husk ash (ARHA), and RH after adsorption samples in figure (1 a, b, c, and d) depict the essential peaks of the unprocessed and processed rice husk. The unprocessed rice husk ash infrared spectrum included intensive bands of absorption at (3,431, 2,925, 1645, 1,082, 769, and 469  $\text{cm}^{-1}$ ). The peak of adsorption that is around (3,431  $\text{cm}^{-1}$ ) reveals the hydroxyl groups' existence. The characteristic of absorption bands at (2,925)  $\text{cm}^{-1}$  was correlated to vibrations of the  $-\text{C}-\text{H}$  stretching of methylene groups, and the vibration of the  $\text{C}=\text{C}$  stretching at (1,645  $\text{cm}^{-1}$ ) shows the aromatic functional groups. The obvious ultimate at (1,082)  $\text{cm}^{-1}$  with a great intensity was ascribed to stretching vibrations of siloxane groups. Peaks around 769 and 469  $\text{cm}^{-1}$  matched to the hydrogenated amorphous silicon (Si-H) [23]. The silanol (OH) groups and the adsorbed water were denoted via a wideband between (3431  $\text{cm}^{-1}$ ) and (2856  $\text{cm}^{-1}$ ). Beyond the thermal processing, the volatile material loss also raises and provides the further porous and loose laky ( $\text{SiO}_2$ ) morphological structure that is effective owing to its great surface area found due to its nano size. The high-temperature effect was noticed upon the spectrum of (FTIR) of the processed sample of rice husk if the spectrum at (2,925  $\text{cm}^{-1}$ ) vanished in all samples which exhibits the ( $\text{CO}_2$ ) development at elevated temperatures and likely disintegration of the remaining methylene group [24]. In the meantime, the other essential peaks of rice husk are still present with a small shift of wavelength.

In the activation of the rice husk ash with (HCL) in figure (1 c), the treatment method didn't disturb the cellulose crystallinity but even improved this structure. The lignin associated groups in four samples could be found at 1662-1633 $\text{cm}^{-1}$ . The  $\text{C}=\text{O}$  group at (1645  $\text{cm}^{-1}$ ) was proposed to conjugate with the aromatic structure from aldehydes and ketones from the lignin. Whereas, the steeper band at around 1101  $\text{cm}^{-1}$  (Figure 1 b, c, and d) is ascribed to the Si-O-Si dissymmetric extending. In figure (1d) of (RH) after adsorption, the ultimate displacement reduction describes the variation in structure with the phosphate, indicating that associated functional groups being in charge with the adsorption process, and the peaks at 804  $\text{cm}^{-1}$  and around it is associated with the phosphate anion group and in figure (1 b, c) with Si-O-Si, respectively. All peaks defined above are related to the mineralogical composition of the sorbent ( $\text{PO}_4$ ,  $\text{SiO}_2$ , and  $\text{CO}_3$ ) [25].

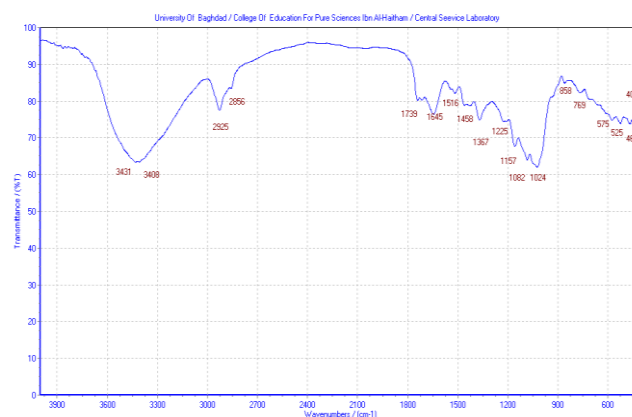
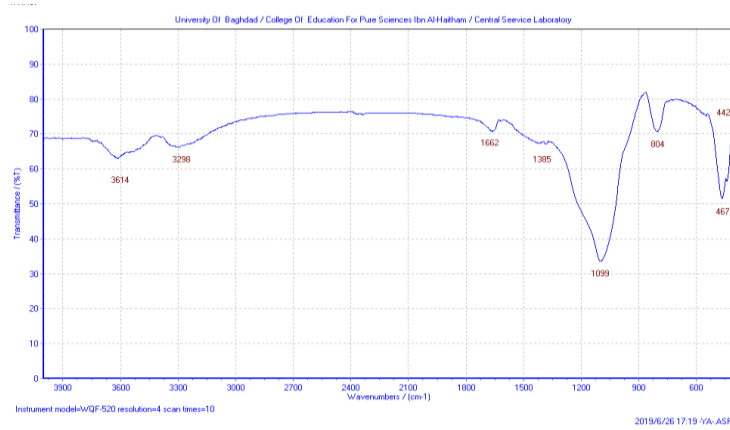
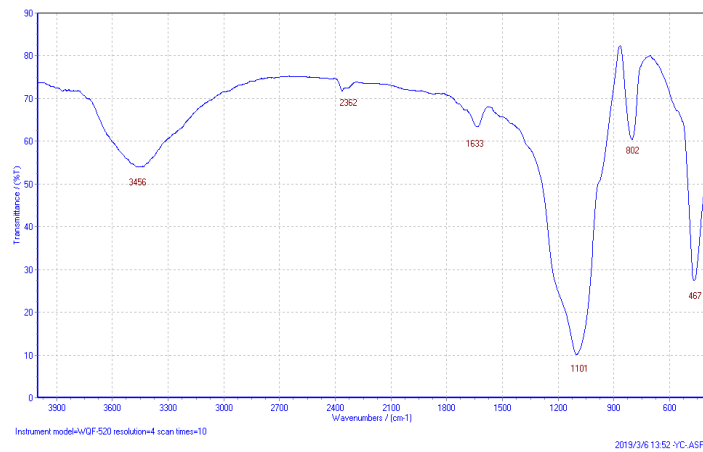


Figure (1a): FTIR spectra of RH.



**Figure (1b): FTIR spectra of RHA.**



**Figure (1c): FTIR spectra of ARHA**

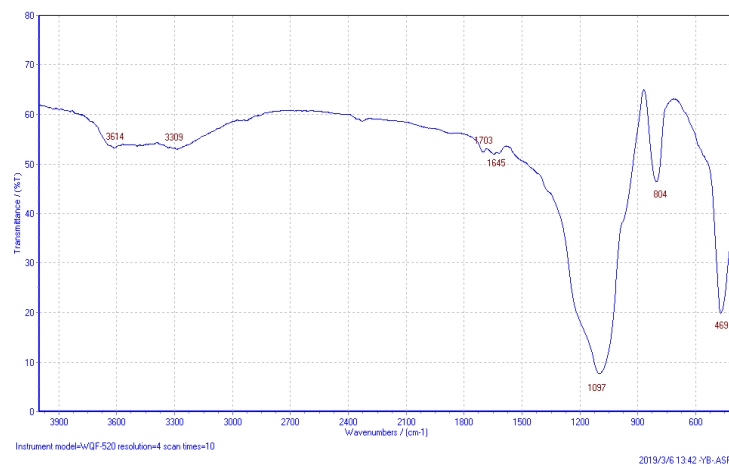


**Figure (1d): FTIR spectra of phosphate after adsorption by RHA.**

The chemical composition of RH and RHA were analyzed by X-ray fluorescence method, as shown in Table (1). SiO<sub>2</sub> occupied maximum quantity, where RHA contains SiO<sub>2</sub> (90.72 %), and RH includes SiO<sub>2</sub> (87.015 %). Other oxides, like (Na<sub>2</sub>O, MgO, K<sub>2</sub>O, CaO, and SO<sub>3</sub>) are existent in minor amounts.

**TABLE I: The adsorbent composition obtained by (X-ray) fluorescence method**

No.	Elemental composition	RH in Percentage %	RHA in Percentage %
1	SiO <sub>2</sub>	87.015	90.72
2	Na <sub>2</sub> O	2.539	0.988
3	MgO	0.502	0.436
4	Al <sub>2</sub> O <sub>3</sub>	0.164	0.0818
5	P <sub>2</sub> O <sub>5</sub>	0.492	0.745
6	K <sub>2</sub> O	0.557	0.5738
7	CaO	8.183	5.782
Λ	<b>SO<sub>3</sub></b>	<b>0.1746</b>	<b>0.297</b>

The surface morphology of the Iraqi rice husk as well as the ash of the Iraqi rice husk was determined employing Scanning Electron Microscope (SEM), and the resulted images are displayed in figure (2 a, b). The rice husk SEM image in figure (2a) views the RH morphology indicating the existence of an agglomerated structure form, slightly porous, and coarse surface. From the other side, the rice husk ash SEM image in figure (2b) reveals the rice husk ash morphology at 500°C. The big agglomerations of various forms and sizes could be noted in comparison with the rice husk in figure (2a). Depending on the micrograph, the large agglomerations were formed from the RH structure disintegration via heat and transformed into slight particles with a big surface area. The micrograph that corresponds to the calcination at a high temperature of (500°C), the micropore volume loss is perhaps ascribed to the collapse of pore and depicted the big holes remaining upon the external epidermis of husks [26]. Energy dispersion X-analysis (EDAX) was performed on the specimens as shown in figure (2), the peaks from the EDAX graph indicate the Iraqi rice husk composed of O2 (RH 41.1 %, RHA 52.7%), C (RH 40.1%, RHA 7.3%), N (RH 13.5%, RHA 0%), and Si (RH 4.3%, RHA 37.2%). The decrease in the C and N percent and the increase in Si are due to the high temperature (500oC) that leads to RHA material.

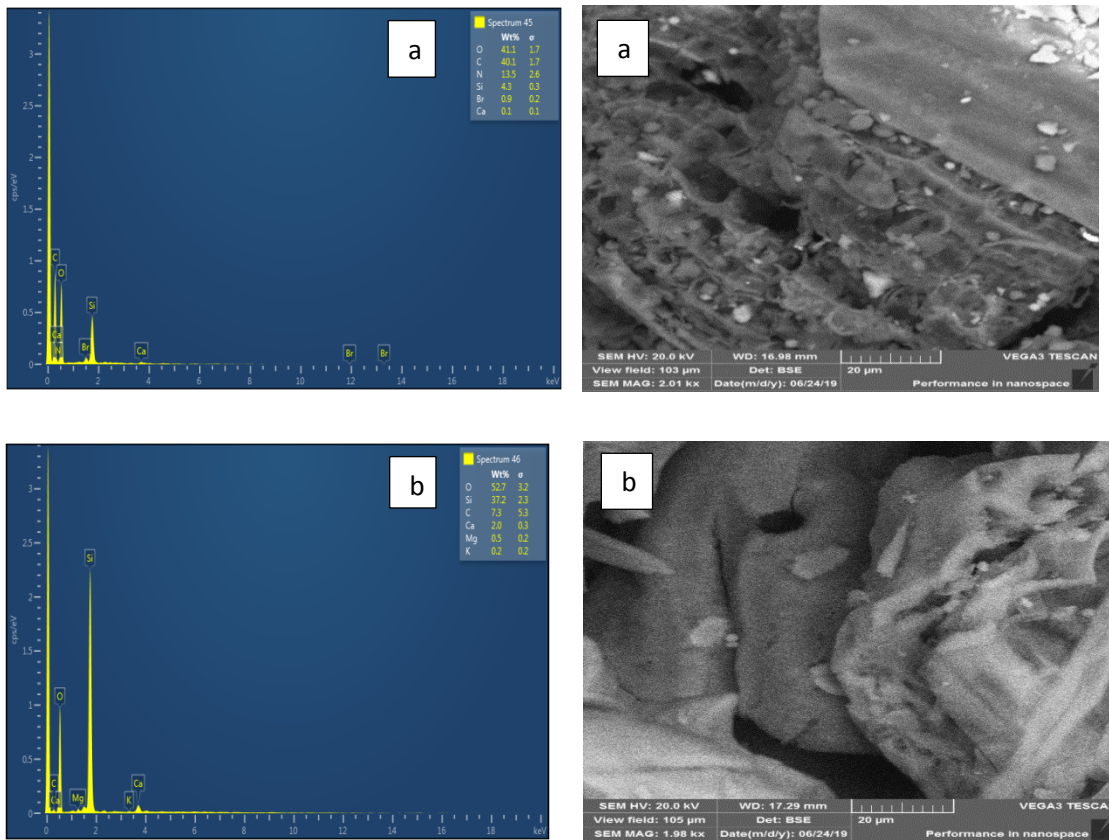


**Fig. (2): Typical EDAX image for (a) RH, (b) RHA. Fig. (2): Typical SEM image for (a) RH, (b) RHA.**

The features of the surface, like the volume of pore and specific surface area, are too significant parameters that must be investigated, because such parameters highly affect the capability of adsorption of an adsorbent.

The BET surface area and the volume of the pore of RH, as well as RHA measured, are briefed in Table (2). The rice husk ash showed an improvement of surface area and pore volume of  $240 \text{ m}^2/\text{g}$  and  $0.2713 \text{ cm}^3/\text{g}$ , respectively compared to the rice husk without processing at  $0.8332 \text{ m}^2/\text{g}$ ,  $0.0041 \text{ cm}^3/\text{g}$ .

The big surface area of the thermally processed rice husk ash was hypothesized for improving the microporosity and narrow the distribution of the pore size. Also, the same tendency was observed via [27] when their results found that the rice husk micropore structure heated at ( $500^\circ\text{C}$ ) was damaged via collapsing or combining both. The specific surface area of thermally processed rice husk rose with the increment of temperature and can be clarified via the development of fresh micro as well as mesopores throughout thermal processing [28].

**TABLE II: Physical properties for RH and RHA**

Adsorbent	Surface Area ( $\text{m}^2/\text{g}$ )	Pore Volume ( $\text{cm}^3/\text{g}$ )
<i>RH</i>	0.8332	0.0041
<i>RHA</i>	240.5406	0.2713

The structure of the RH and RHA were investigated by X- diffraction and the state was revealed by the shape of the XRD patterns obtained. The X-Ray diffraction of RH and RHA is displayed in figure (3 a, b). In figure (3 a), the XRD scans were recorded from  $10 - 80^\circ$ . The strongest peak was noticed at ( $2\theta = 22^\circ$ ) which is a featured peak of the amorphous silica. This depicts the crystalline nature of silica and the existence of the group of Si-O-Si. From the other side, figure (3 b) shows the analysis of (XRD) of (RHA) and showed that the quartz is the merely crystalline phase exists in ash, and the quartz source may be ascribed to a single of or a combination of these factors: pollution via windblown sand, conveyed into the plant via the sap, and silica crystallization at the temperature of calcination [29].

The results revealed that (RH) and (RHA) are amorphous substance aspects, the (RH) heating at ( $500^\circ\text{C}$ ) didn't vary the amorphous silicon dioxide structure to a crystalline structure (noticed at  $2\theta = 22^\circ$ ). Also, the results obtained in the present work are in good agreement with the results obtained by [29, 30].

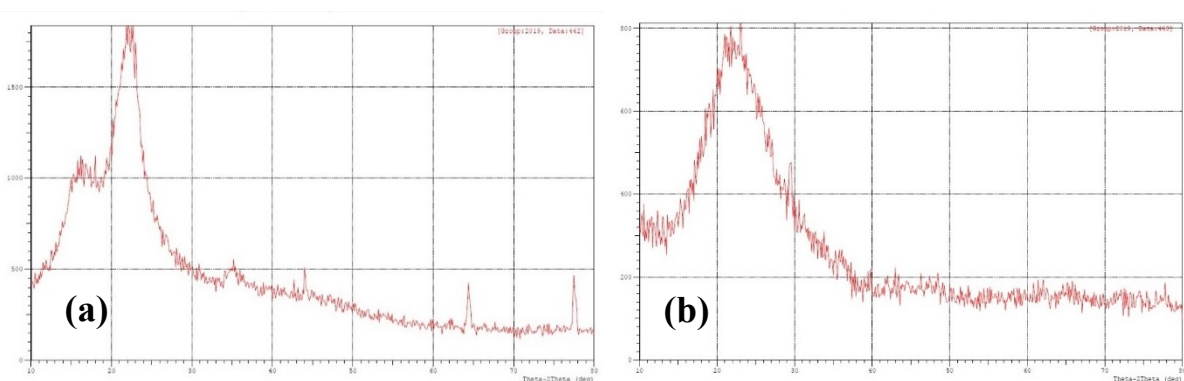


**Figure (3): (a) XRD patterns of RH. (b) XRD patterns of RHA.**

## ***II. Influence of various treatments of rice husk upon the efficiency of removal***

Different treatments of rice husk were made to examine the capability of the rice husk for the adsorption of phosphate anion from its solution, and the following results come into view by the figure (4):

1) The figure indicates that the rice husk (RH) has a weak ability of removal (16.95%) to adsorb the phosphate anion among the different types of treatments, and the crushed rice husk (CRH) gives a higher removal (20.34%) comparing with the RH. The increase in the removal of CRH (20.34%) belongs to the increasing of surface area, and that means increasing in active site in CRH which leads to adsorb the phosphate anion.

2) The removal in thermally treated rice husk (TTRH) (43.56 %) is too high compared with the rice husk (RH) (16.95%), because of the high surface area of TTRH is that obtained at treated the rice husk at 400 °C.

The maximum removal in TTRH (43.56 %) among the different treatments of rice husk for phosphate anion adsorption leads to use the of TTRH as a good adsorbent in this treatment.

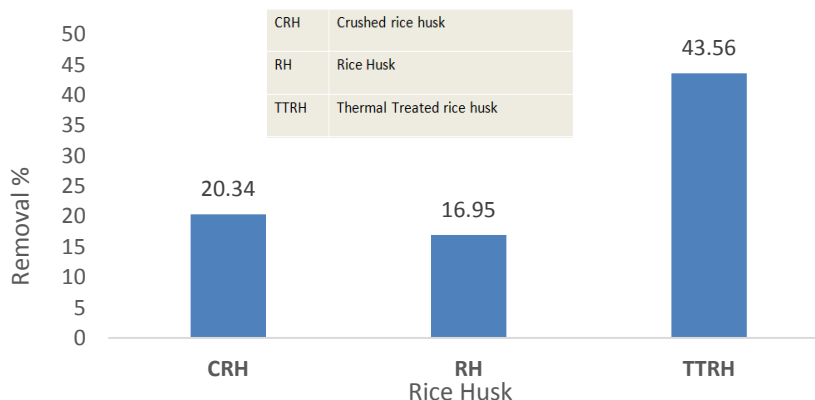


**Figure (4): Comparison between rice husk, crushed rice husk, and thermal treated rice husk upon the removal efficiency of phosphate anion (Contact time = 140 min., Dose = 0.5 gm,  $C_0 = 30$  mg/L, at room temperature).**

### III. Effect of Temperature on Rice Husk

The results regarding the effect of heat treatment of rice husk at different temperatures on the adsorption of phosphate anion are shown in figure (5). The results indicated that the phosphate anion adsorption rises with the increment in temperature from 300 to 500°C with the efficiency of removal from 77.19% to 94.74% and then decreases. So, the phosphate anion adsorption was desirable at the temperature 500°C with maximum removal of 94.74%. It was observed from figure 5 that the ash gained at a lower temperature (300, 400°C) of burning than (500°C) possesses some unburned carbonaceous substance. The volatile substance, like hemicelluloses, cellulose, and lignin, also don't burn totally at such lower temperature and therefore demonstrates certain crystallinity. The volatile matter such as lignin, cellulose, hemicelluloses also do not burn completely at this lower temperature and hence shows some crystallinity. If rice husk is burnt at a controlled temperature, throughout the thermal disintegration of the organic substance, it will leave very porous and nanostructured particles of silica. When the heating temperature rises, the volatile substance loss also raises. That provides the highly porous and loose flaky morphological structure of (SiO<sub>2</sub>) that is effective owing to its high surface area gained due to its nano size. The flaky morphology of the rice husk proposes that the surface is further loosely bound which creates it more amorphous and reactive [31].

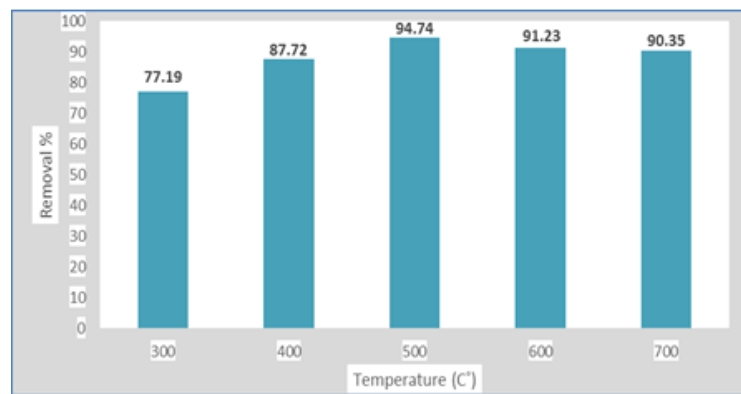


**Figure (5): Effect of Different Burning Temperatures of rice husk upon the removal efficiency of phosphate anion ( $C_0 = 30$  mg/L, Contact time = 140 min., Dose = 1 gm, pH = 2, at room temperature).**

#### **IV. Effect of time of contact**

The phosphate removal was investigated employing fabricated wastewater including (30 ppm) of the solution of phosphate. The phosphate adsorption utilizing (RHA) was studied by changing the time of contact (5-200 min) and the dose of adsorbent (0.5 gm) at the room temperature and (250 rpm) of agitating speed.

The contact time influence upon the phosphate anion removal is shown in figure (6). The removal percentage of phosphate anion by RHA increases gradually during the range (5-100) min, then the removal is rapid from (120) to (140) min of the contact period and then decreases. The maximum removal percentage of phosphate anion was 63.92 % in 140 min. This result depicted that the adsorption rate is greater at the commencement and owing to the readiness of a big no. of effective sites upon adsorbent. When such sites are fatigued, the uptake rate is governed via the rate, at which the adsorbate is conveyed from external to internal sites of the adsorbent particles [32]. The ultimate removals were reached within the first (140) min stirring time. There mustn't be appeared to be more advantages beyond (150 min). So, the time of stability was fixed (140) min in further experiments.

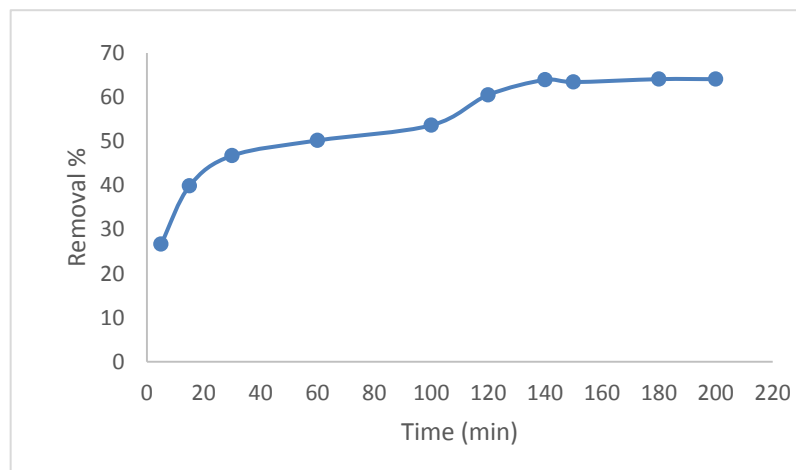


**Figure (6): Influence of time upon the adsorption removal of phosphate anion ( $C_0 = 30$  mg/L, pH = 7, adsorbent dose = 0.5 g, at room temperature).**

#### **V. Influence of (pH) solution upon the adsorption of phosphate**

The phosphate solution pH magnitude is a significant monitoring parameter in the process of adsorption since the amount of ionization and speciation of adsorbate is chiefly influenced via the solution (pH) value [21].

The phosphate removal was investigated utilizing fabricated aqueous solution comprising (30) ppm of the phosphate and reaching the (pH 2). The outcomes revealed that the removal percentage reduces with the increment within the solution pH as clarified in figure 7. The ultimate removal till 98.28 % was noticed at (pH 2), which indicates that the removal of phosphate is highly effective in

an acidic state and it drops with the increment in the solution (pH). Therefore, the whole additional investigations upon the phosphate removal were conducted via a (6 pH) solution.

Also, former investigations manifested that with the increment in the (pH), adsorbent removal efficiency decreases. Large (pH) causes the functional group's separation thus conveys further negative ions that withstand the interacting of the phosphate ions with the surfaces, hence reducing the phosphate adsorption [33]. At lower (pH), the attraction of positive ions towards the phosphate ions to form the stable ion is more, hence the (pH) of the solution also affects the removal percentage of phosphate [8].

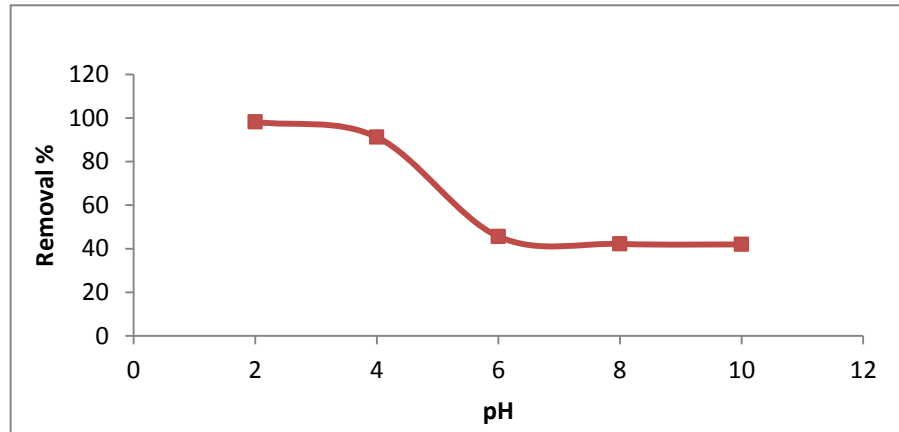


Figure (7): Influence of (pH) upon the removal efficiency of phosphate anion ( $C_0 = 30$  mg/L, Contact time= 140 min., Dose=0.5 gm, at room temperature).

Points of zero charge (PZCs) are the pH magnitudes at which the surface charge components are equal to (0) beneath the certain temperature states, the applied pressure, and the aqueous solution composition [34]. This doesn't mean the surface possesses no charge at the ( $pH_{PZC}$ ), but rather there're equal quantities of negative and positive charges. The (PZC) magnitudes could assist to optimize the substrate choice for the process contaminants. Substrates with low (PZC) magnitudes would be the best suited for treating the effluents that are contaminated with the cations, whereas the substrates with high (PZC) magnitudes of (PZC) would be highly suitable for arresting the anions. The zero charge pH point ( $pH_{PZC}$ ) investigation either verifies the increment of the phosphate elimination with a pH around (2). The (pH) at the zero charge point ( $pH_{PZC}$ ) of arranged (RHA) was obtained via the technique of the solid addition. The material ( $pH_{PZC}$ ) in a solution is the magnitude of pH, at which the net surface charge of this material is equal to (0), beneath such pH (the  $pH=9$  in the current investigation, as depicted in figure 8). The adsorbent functional group is protonated, and the adsorbent surface is completely charged; nevertheless, the adsorption of negatively charged ions is preferred. In the simplest explanation, the  $H^+$  ions are the winners in such competition. Beyond such pH, such groups deprotonate, and the adsorbent surface is negatively charged, hence within such zone of pH, the phosphate ions cannot be actively attracted upon the surface of (RHA) [35].

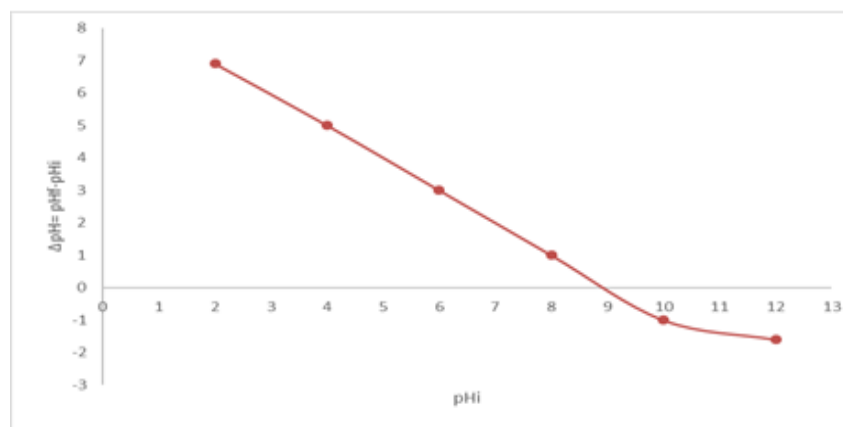


Figure (8): pH point of zero charges ( $pH_{PZC}$ )

## VI. The influence of adsorbent dose

The adsorbent dose influence upon the removal of phosphate from the phosphate solution is illustrated in figure 9. It evinces that the removal percent of phosphate in the solution rose with the increasing of the adsorbent dose for a given primary concentration of phosphate. This outcome was expected since raising the adsorbent doses gives a larger surface area owing to the increment in the number of the effective sites of the adsorbent.

Via raising the adsorbent mass by (2, 6, and 10 g/L), the efficiency of phosphate removal raised by (81.1%, 93.9%, 94.67%), respectively and via raising the adsorbent mass from (10) to (14 g/L), the efficiency of removal rose slightly till (96 %) (20 g/L) and the maximum capacity is (1.44 mg/g). So, above (20 g/L) of the mass of adsorbent, the phosphate removal percentage was almost fixed, this could be ascribed to the truth that by raising the quantity of adsorbent for the similar phosphate ion concentration, the number of the effective site accessible for the phosphate uptake raises, but a stage arises afterward in which the removal reaches its ultimate limit and more increment in the dose did not influence as before proposed by [14].

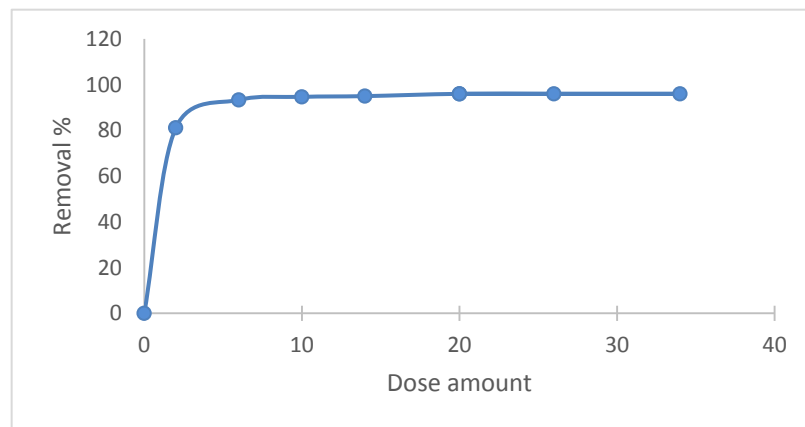


Figure (9): Influence of the adsorbent dose upon the removal efficiency of phosphate anion ( $C_0 = 30$  mg/L, Contact time = 140 min., pH=2, at room temperature)

## VII. The influence of primary of phosphate concentration

The primary concentration provides an essential force of motivation for overcoming phosphate ion transfer resistance in the solid-liquid interface. For determining primary concentration influence upon the removal of phosphate, the experiment was performed utilizing (9) series of concentration of phosphate (5–150 mg/L) with a constant quantity of the (RHA) dosage; 20 g/L and pH=2. The outcome determined is exhibited in figure (10). Generally, the removal percentage of phosphate in the wastewater reduced with the raised primary concentration of phosphate. At the minimum utilized concentration (5 mg/L), of phosphate, the removal of phosphate till (98.37 %). Nonetheless, if the primary concentration was raised till (150 mg/L), the removal decreased to (32.75%) and the maximum experimental capacity is 2.78 mg/g. This is due to the deficiency of binding sites in the RHA sample for the phosphate anions adsorption at higher concentrations. The effect of primary phosphate concentration could be clarified as follow: at minimum phosphate anion/adsorbent ratio, phosphate anion adsorption includes higher energy binding sites. As the phosphate anion/adsorbent ratio raise (i.e., at higher primary concentration), the higher energy binding sites are saturated and adsorption starts on lower energy binding sites, resulting in a decrease in the adsorption efficiency [36].

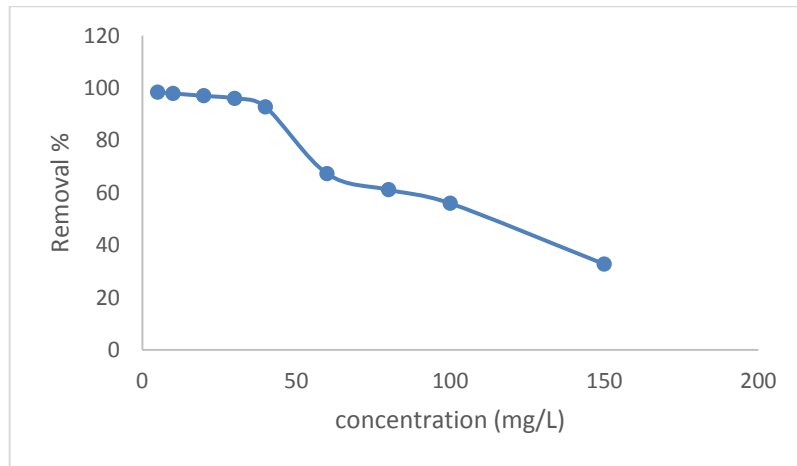


Figure (10): Effect of Initial Concentration on the removal efficiency of phosphate anion (Dose adsorbent = 20 g/L, pH =2, Contact time= 140 min., at room temperature).

VIII. Effect of competitive anions

In the current work, the plurality of the tests was finished with just phosphate anions yet; in the natural system, a few different anions are available which can compete with phosphate. The effects of various competing anions ( $SO_4^{-2}$ ,  $NO_3^{-}$  and  $CO_3^{-2}$ ) were studied on the uptake of phosphate by RHA, as shown in (Fig. 12).

Various competing anions used the same amount of concentration and 5X equivalent concentration of phosphate in order to determine the phosphate selectivity. The amount of phosphate uptake decreased with the presence of other anions ( $SO_4^{-2}$ ,  $NO_3^{-}$  and  $CO_3^{-2}$ ). From the other side, the  $CO_3^{-2}$  existence abruptly reduced the quantity of the uptake of phosphate, and the existence of sulfate anion showed a little effect on the phosphate uptake, as shown in Figure 11.

The effects of competing anions on the phosphate adsorption by RHA was found to follow this sequence  $CO_3^{-2} > NO_3^{-} > SO_4^{-2}$ , these results demonstrated that the RHA could be a good material for  $CO_3^{-2}$  anion and  $NO_3^{-}$  anion removal [37]. It is worth mentioning that conducting an experiment on a real application, for example, a sample of kitchen waste using detergents can be studied in future work.

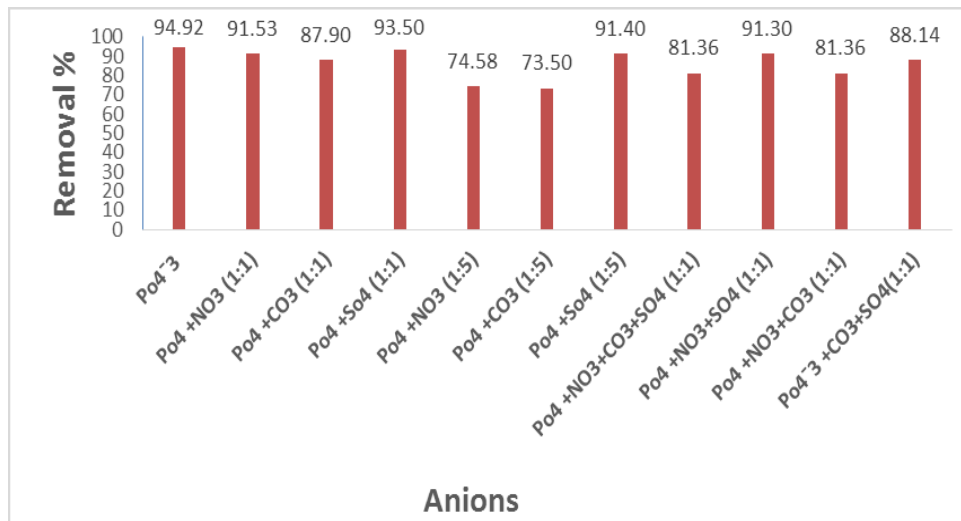


Figure (11): Effect of the other anions on phosphate anion adsorption in presence of RHA adsorbent.

IX. Adsorption Isotherm

The constants and the nonlinear reversion coefficient of resolution ( $R^2$ ) for the three isotherms are given in Table (4) and the experimental data fitted well to all the isotherm models Langmuir, Freundlich and Temkin as shown in the figure (12).

The models Langmuir and Temkin are best for the results research but the best is Langmuir. Langmuir isotherm display for RHA gave the best fitting to the trial information. The coefficient of determination ( $R^2= 0.99$ ) was gotten.

The circumstance of  $n > 1$  is most normal and might be because of the surface sites organization or any factor, which leads to a diminishing in the interaction of adsorbent adsorbate with expanding the density of surface [38], and the estimations of ( $n$ ) inside the range of (1–10) show preferred adsorption [39, 40].

The ( $n$ ) magnitude of the Freundlich isotherm model for the uptake of phosphate via the rice husk was more than unity, as depicted in Table 4.4, which denotes to an adsorption intensity and a heterogeneous surface with the least interactions between the exchange sites in the adsorbent and the phosphate anions [41].

TABLE III: Adsorption kind according to value of n

Value of n	Kind of adsorption
n=1	Linear
n>1	Physical Process
n<1	Chemical Process

TABLE IV: Isotherm parameters for phosphate anion adsorption by RHA

Langmuir		Freundlich				Temkin					
$q_{exp}$ mg/g	$q_m$ (mg/g)	$K_L$ (L/g)	$R^2$	$R_L$	$K_f$ ( $mg^{1-n}$ $g^{-1} L^n$ )	$1/n$	$n$	$R^2$	$B$ (J/mol)	$K_t$ (L/g)	$R^2$
2.7	2.5	1.002	0.99	0.032	1.21	0.22	4.5 3	0.86 8	0.3353	37	0.92

To predict the favorability of an adsorption system, the Langmuir equation can also be expressed in terms of a dimensionless separation factor or an equilibrium parameter  $R_L$ . Table (4) shows the  $R_L$  values based on the Langmuir isotherm model, in which all  $R_L$  values are greater than (0) but less than 1 indicating that the Langmuir isotherm is favorable.

The experimental capacity is 2.7 mg/g and the maximum capacity is 2.5, that is, the confirming between the experimental and maximum capacity.

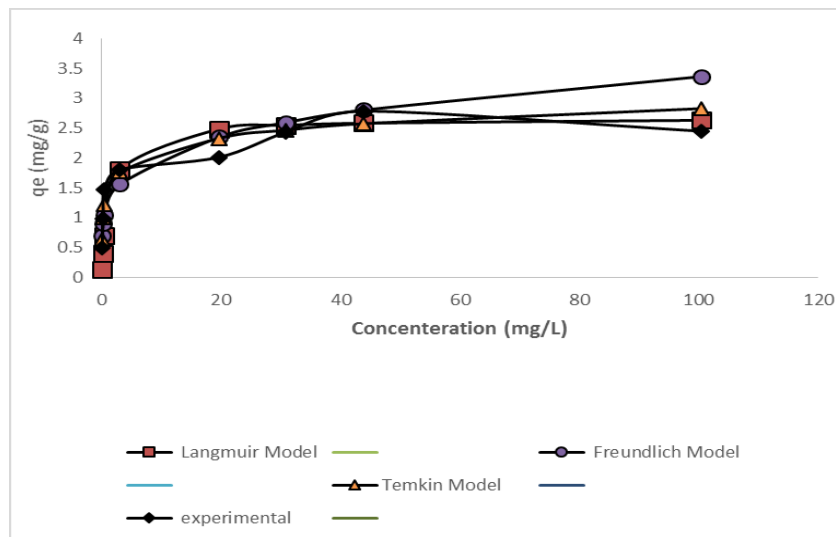


Figure (12): Experimental, Langmuir, Freundlich and Temkin adsorption isotherms of Phosphate anion onto RHA adsorbent at room temperature

### X. Adsorption Kinetic Study

To examine the kinetics of phosphate anion adsorption on RHA, kinetic models pseudo-first-order and pseudo-second-order were used. The active parameters of the two models are exhibited in Table (5) and the experimental data fitted well to the kinetic models pseudo-first-order and pseudo-second-order as shown in the figure (13).

The obtained results from both models for the adsorption of phosphate by RHA are listed in Table (5), with the magnitudes of the pseudo-first-order and second-order expression parameters with the coefficients of correlation. The pseudo-second-order kinetic model supplied the best fit to the experimental data. The coefficient of determination ( $R^2$ ) was 0.99, and the computed magnitudes of  $q_e$  were too near to the experimental magnitudes ( $q_e$  (exp.)).

TABLE V: Parameters of kinetic models for phosphate anion adsorption by RHA

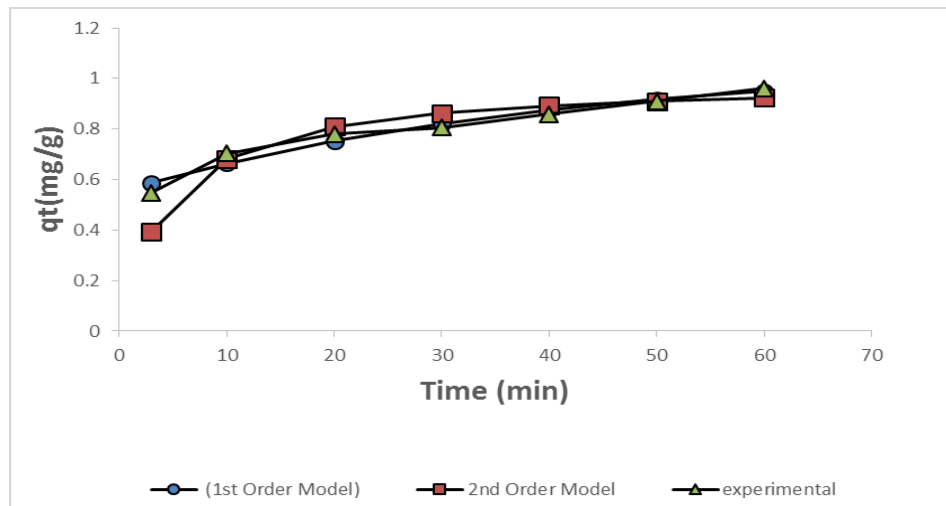


Figure (13): Kinetic Model, 1<sup>st</sup> order, 2<sup>nd</sup> order, and experimental of Phosphate anion onto RHA adsorbent ( $C_0=30$  mg/L, dose= 1 gm, pH=2, and 25 C°)

## 4. CONCLUSION

The rice husk is an agricultural waste that is locally accessible within a big amount. The current work adsorbent demonstrates its effectiveness to be attractive for the phosphate processing from the aqueous solution. The result elucidated that the thermally processed rice husk at 500 C° improved the capacity of the phosphate adsorption and manifested the ultimate removal and capacity respectively 98.37% and 1.44 mg/g of phosphate at contact time= 140 min., pH = 2, utilizing (20 g/L) dose, and initial concentration 5 mg/L. The data of the equilibrium adsorption evinced the best fit for the Langmuir isotherm model ( $R^2 = 0.99$ ) and the pseudo-second-order kinetic model ( $R^2 = 0.99$ ). The analysis of (XRF) displayed the silica existence, while the (FTIR) and (XRD) investigation depicted the existence of the crystalline silica and (Si-O-Si) group. The SEM showed the (ARHA) morphology of the RHA (rice husk burnt at 500 C°) and large agglomerated of different sizes and shapes could be observed. The result of the present investigation proposes that the burnt rice husk at 500°C gives the best result for the phosphate anion adsorption and proposes that the rice husk ash possesses the potential to be utilized as a low-cost adsorbent for the treatment of water and wastewater. Additionally, using the Iraqi waste rice husk-based adsorbent will also resolve its discarding problem.

Adsorbent	$q_e$ exp. (mg/g)	Pseudo-first-order			Pseudo-Second-order		
		$q_e$ (Cal.) (mg/g)	$K_1$ ( $min^{-1}$ )	$R^2$	$q_e$ (cal.) (mg/g)	$K_2$ (gm/mg.min)	$R^2$
RHA	1.06	0.91	0.025	0.97	0.92	0.192	0.99

**References:**

- [1] P.R. Rout, P. Bhunia, and R.R. Dash, "Modeling isotherms, kinetics and understanding the mechanism of phosphate adsorption onto a solid waste: Ground burnt patties", *Journal of Environmental Chemical Engineering*, 2(3), pp. 1331–1342, 2014.
- [2] E. Oguz, "Thermodynamic and kinetic investigations of  $\text{PO}_4^{3-}$  adsorption on blast furnace slag", *Journal of Colloid and Interface Science*, 281, pp. 62–67, 2005.
- [3] Z. Wang, D. Shen, F. Shen, and T. Li, "Phosphate adsorption on lanthanum loaded biochar", *Chemosphere*, 150, pp. 1–7, 2016.
- [4] J. Zhang, Z. Shen, W. Shan, Z. Mei, and W. Wang, "Adsorption behavior of phosphate on lanthanum(III)-coordinated diamino-functionalized 3D hybrid mesoporous silicates material", *Journal of Hazardous Materials*, 186, pp. 76–83, 2011.
- [5] S. Mor, K. Ravindra, De Visscher, A., R.P. Dahiya, and A. Chandra, "Municipal solid waste characterization and its assessment for potential methane generation: a case study", *Science of the Total Environment*, 371(1), pp. 1-10, 2006a.
- [6] S. Mor, K. Ravindra, R.P. Dahiya, and A. Chandra, "Leachate characterization and assessment of groundwater pollution near municipal solid waste landfill site", *Environmental and Monitoring Assessment*, 118(1-3), pp. 435-456, 2006b.
- [7] T. Wium-Andersen, A.H. Nielsen, T. Hvitved-Jacobsen, H. Brix, C.A. Arias, and J. Vollertsen, "Modeling the eutrophication of two mature planted stormwater ponds for runoff control", *Ecological Engineering*, 61, pp. 601–613, 2013.
- [8] S. Mor, K. Ravindra, and N.R. Bishnoi, "Adsorption of chromium from aqueous solution by **activated alumina** and activated charcoal", *BIORESOUR Technol*, 98(4), pp. 954-957, 2007.
- [9] K. Ravindra, K. Kaur, and S. Mor, "System analysis of municipal solid waste management in Chandigarh and minimization practices for cleaner emissions", *Journal of Cleaner Production*, 89, pp. 251-256, 2015.
- [10] M. Oliveira, A. V, and R. Nogueira, "Phosphorus Removal from Eutrophic Waters with an Aluminium Hybrid Nanocomposite", *Water, Air, & Soil Pollution*, 223(8), pp. 4831–4840, 2012.
- [11] T. Park, V. Ampunan, S. Maeng, and E. Chung, "Application of steel slag coated with sodium hydroxide to enhance precipitation-coagulation for phosphorus removal", *Chemosphere*, 167, pp. 91–97, 2017.
- [12] X. Xu, B. Gao, W. Wang, Q. Yue, Y. Wang, & S. Ni, "Adsorption of phosphate from aqueous solutions onto modified wheat residue: characteristics, kinetic and column studies", *Colloids and Surfaces, B, Biointerfaces*, 70(1), pp. 46–52, 2009.
- [13] M. Rathod, K. Mody, & S. Basha, "Efficient removal of phosphate from aqueous solutions by red seaweed", *Kappaphycus alvarezii*, *Journal of Cleaner Production*, 84, pp. 484–493, 2014.
- [14] D. Yadav, M. Kapur, P. Kumar, and M.K. Mondal, "Adsorptive removal of phosphate from aqueous solution using rice husk and fruit juice residue", *Process Safety and Environmental Protection*, 94, pp. 402–409, 2014.
- [15] J. Torit, & P. Doungkamon, "Phosphorus removal from wastewater using eggshell ash", *Environmental Science and Pollution Research*, pp. 1-9, 2018.
- [16] W. Chansuvarn, "Removal of Phosphate from Wastewater Using Carbonized Filter Cake", *Division of Science, Faculty of Science and Technology, Rajamangala University of Technology Phra Nakhon, Bangkok 10800, Thailand*, *Applied Mechanics and Materials Submitted: ISSN: 1662-7482, Vol. 879*, pp. 125-130, 2017.
- [17] A.K. Babayemi, "Performance Evaluation of Palm Kernel Shell Adsorbents for the Removal of Phosphorus from Wastewater", *Advances in Chemical Engineering and Science*, 7, pp. 215-227, 2017.
- [18] M.C. Manique, C.S. Faccini, B. Onorevoli, E.V. Benvenuti, and E.B. Caramão, "Rice husk ash as an adsorbent for purifying biodiesel from waste frying oil. *Fuel*", 92(1), pp. 56–61, 2012.
- [19] S.M. Gawande, K. Shelke, N.A. Dhoke, M.D. Lengre, and A.D. Diksha, "Analysis and removal of phosphate from wastewater by using rice husk", *International Research Journal of Engineering and Technology (IRJET)*, Vol. 04, pp. 2115-2119, 2017.
- [20] S. Mor, K. Chhoden, and R. Khaiwal, "Application of Agro-waste Rice Husk Ash for the Removal of Phosphate from the Wastewater", *Journal of Cleaner Production*, Vol. 129, pp. 673-680, 2016.

- [21] S. Hamzah, N.A. Razali, N.I. Yatim, M. Alias, A. Ali, N.S. Zaini, and A.A.M. Abuhabib, "Characterisation and performance of thermally treated rice husk as efficient adsorbent for phosphate removal", *Journal of Water Supply: Research and Technology*, Vol. 67, pp. 766-778, 2018.
- [22] S. Pradhan, and M.R. Pokhrel, "Spectrophotometric Determination of Phosphate in Sugarcane Juice, Fertilizer, Detergent and Water Samples By Molybdenum Blue Method", *Central Department of Chemistry, Tribhuvan University, Kiritipur, Kathmandu, Nepal*, Vol. 11(11), pp. 58-62. 2013.
- [23] K.P. Dey, S. Ghosh, and M.K. Naskar, "Organic template-free synthesis of ZSM-5 zeolite particles using rice husk ash as silica source", *Ceramics International*, 39(2), pp. 2153-2157, 2013.
- [24] K. Kudaibergenov, Y. Ongarbayev, Z.A. Mansurov, and D. Yerlan, Study on the effectiveness of thermally treated rice husks for petroleum adsorption, *Journal of Non-Crystalline Solids*, 358 (22), pp. 2964-2969, 2012.
- [25] D.S. Soejoko, M.O. Tjia, "Infrared spectroscopy and X-ray diffraction study on the morphological variations of carbonate and phosphate compounds in giant prawn (*Macrobrachium Rosenbergii*) skeletons during its moulting period", *Journal of Materials Science*, Vol. 38, pp. 2087-2093, 2002.
- [26] S.B. Daffalla, H. Mukhtar, and M.S. Shaharun, "Characterization of adsorbent developed from rice husk: effect of surface functional group on phenol adsorption", *Journal of Application Science*, Vol. 10(12), pp. 1060-1067, 2010.
- [27] T.H. Liou, and S.J. Wu, "Characteristics of microporous/mesoporous carbons prepared from rice husk under base-and acid-treated conditions", *Journal of Hazards Materials*, Vol. 171 (1-3), pp. 693-703, 2009.
- [28] D. Kalderis, S. Bethanis, P. Paraskeva, and E. Diamadopoulos, "Production of activated carbon from bagasse and rice husk by a single-stage chemical activation method at low retention time", *Bioresour. Technology*, Vol. 99 (15), pp. 6809-6816, 2008.
- [29] R. Jauberthie, F. Rendell, S. Tamba, and I. Cisse, "Origin of the pozzolanic effect of rice husks", *Construction Building Materials*, Vol. 14, pp. 419-423, 2000.
- [30] A. Imyim and E. Prapaimrunsi, "Humic Acids Removal from Water by Aminopropyl Functionalized Rice Husk Ash", *Journal of Hazardous Materials*, 184(1-3), pp. 775-781, 2010.
- [31] D. Pallavi, P. Dilip, and P. Shaikumar, "FTIR and TGA analysis in relation with the % crystallinity of the SiO<sub>2</sub> obtained by burning rice husk at various temperatures", *Advanced Materials Research*, Vol. 585, pp. 77-81, 2012.
- [32] K. Vijayaraghavan, Y.S. Yun, "Bacterial biosorbents and biosorption", *Biotechnol Adv*, Vol. 26, pp. 266-291, 2008.
- [33] W. Huang, S. Wang, Z. Zhu, L. Li, X. Yao, V. Rudolph, and F. Haghseresht, "Phosphate removal from wastewater using red mud" *Journal of Hazardous Materials*, 158(1), pp. 35-42, 2008.
- [34] G. Sposito, "The chemistry of soils", 2nd edition, Oxford University Press, New York, 2008.
- [35] B. Zubeyde, C. Ercan, and D. Mehmet, "Equilibrium and thermodynamic studies on biosorption of Pb(II) onto *Candida albicans* biomass", *Journal of Hazard Materials*, Vol. 161, pp. 62-67, 2009.
- [36] Z. Al-Qodah, "Biosorption of heavy metal ions from aqueous solutions by activated sludge", *Desalination*, Vol.196 (1-3), pp. 164-176, 2006.
- [37] B. Thl, "Removal of nitrate from water and wastewater by ammonium-functionalized SBA-16 mesoporous silica", Quebec City, Laval University, 2013.
- [38] B.E. Reed, and M.R. Matsumoto, "Modeling cadmium adsorption by activated carbon using the Langmuir and Freundlich isotherm expressions", *Separation science and technology*, Vol. 28(13-14), pp. 2179-2195, 1993.
- [39] G. Mckay, M.S. Otterburn, and A. G. Sweeney, "The removal of colour from effluent using various adsorbents—III", *Silica: rate processes Water Research*, Vol. 14(1), pp. 15-20, 1980.
- [40] A. Özer, and H.B. Pirincci, "The adsorption of Cd (II) ions on sulphuric acid-treated wheat bran", *Journal of Hazardous materials*, Vol. 137(2), pp. 849-855, 2006.
- [41] S. Bagherifam, S. Komarneni, A. Lakzianb, A. Fotovat, R. Khorasani, W. Huang, J. Ma, S. Hong, F.S. Cannon, and Y. Wang, "Application Clay Science", Vol. 95, pp. 126-132. 2014.